Neuron
Article

Chemical Genetic Identification of NDR1/2 Kinase Substrates AAK1 and Rabin8 Uncovers Their Roles in Dendrite Arborization and Spine Development

Sila K. Ultanir,[1,2,9,*] Nicholas T. Hertz,[1,5,9] Guangnan Li,[6,7] Woo-Ping Ge,[1,2] Alma L. Burlingame,[8] Samuel J. Pleasure,[6,7] Kevan M. Shokat,[1,5] Lily Yeh Jan,[1,2,3,4] and Yuh-Nung Jan[1,2,3,4,*]
[1]Howard Hughes Medical Institute
[2]Department of Physiology
[3]Department of Biochemistry
[4]Department of Biophysics
[5]Department of Cellular and Molecular Pharmacology
[6]Programs in Developmental Biology and Neuroscience, Eli and Edythe Broad Center of Regeneration Medicine and Stem Cell Research
[7]Department of Neurology
[8]Department of Pharmaceutical Chemistry
University of California, San Francisco, San Francisco, CA 94143, USA
[9]These authors contributed equally to this work
*Correspondence: sila.ultanir@gmail.com (S.K.U.), yuhnung.jan@ucsf.edu (Y.-N.J.)
DOI 10.1016/j.neuron.2012.01.019

SUMMARY

Dendrite arborization and synapse formation are essential for wiring the neural circuitry. The evolutionarily conserved NDR1/2 kinase pathway, important for polarized growth from yeast to mammals, controls dendrite growth and morphology in the worm and fly. The function of NDR1/2 in mammalian neurons and their downstream effectors were not known. Here we show that the expression of dominant negative (kinase-dead) NDR1/2 mutants or siRNA increase dendrite length and proximal branching of mammalian pyramidal neurons in cultures and in vivo, whereas the expression of constitutively active NDR1/2 has the opposite effect. Moreover, NDR1/2 contributes to dendritic spine development and excitatory synaptic function. We further employed chemical genetics and identified NDR1/2 substrates in the brain, including two proteins involved in intracellular vesicle trafficking: AAK1 (AP-2 associated kinase) and Rabin8, a GDP/GTP exchange factor (GEF) of Rab8 GTPase. We finally show that AAK1 contributes to dendrite growth regulation, and Rabin8 regulates spine development.

INTRODUCTION

Dendrite arborization is crucial for establishing the complex neural networks in the brain. Dendrites of mammalian hippocampal and cortical pyramidal neurons are covered with dendritic spines, which are sites for >90% of excitatory synapses in the central nervous system (Nimchinsky et al., 2002). Significant progress has been made in understanding the molecular mechanisms that regulate dendrite development in *Drosophila* (Jan and Jan, 2010). Elucidating the mechanisms that control dendrite morphogenesis and spine development in mammals is important, since defects of such mechanisms likely underlie many neurodevelopmental disorders, such as autism and schizophrenia (Penzes et al., 2011; Ramocki and Zoghbi, 2008).

NDR (nuclear Dbf2-related) kinases are a subclass of AGC (protein kinase A (PKA)/PKG/PKC) group of serine/threonine kinases, which include two related kinase families: NDR1/2 and Lats1/2 (large tumor suppressor 1/2; Hergovich et al., 2006). The NDR1/2 kinase pathway's key components, NDR1/2/Tricornered, upstream-activating kinase MST1-3 (Mammalian Sterile 20-like 1-3)/Hippo, cofactor MOB 1/2 (Mps one binder 1/2)/Mats (Mob as tumor suppressor), and scaffold protein FURRY1/2/Furry, are conserved from yeast to mammals (Hergovich et al., 2006). NDR1/2 homologs (Cbk1p in yeast, SAX-1 in worms, and Trc in fly) regulate polarized cellular differentiation in various organisms, including bud formation in yeast (Nelson et al., 2003), epidermal hair tip and sensory bristle formation in *Drosophila* (Cong et al., 2001; Geng et al., 2000), and dendritic morphogenesis and tiling in the worm and fly (Emoto et al., 2004, 2006; Gallegos and Bargmann, 2004; Han et al., 2012). The two Trc homologs mammalian (Stk38) and NDR2 (Stk38l; referred to as NDR1/2) are ~86% identical. Their biochemical activation has been well characterized with no difference between NDR1 and NDR2 reported (Hergovich et al., 2006). NDR1 and NDR2 are broadly expressed in the mouse brain (Devroe et al., 2004; Stegert et al., 2004; Stork et al., 2004). NDR1 knockout mice have increased susceptibility to tumor formation, implicating NDR1 as tumor suppressor (Cornils et al., 2010). NDR2 levels are increased in NDR1 knockout mice and may compensate for the absence of NDR1 (Cornils et al., 2010). The potential roles of NDR1/2 in regulating mammalian neuronal morphogenesis are unknown.

Despite the importance of the NDR1/2 kinase pathway in regulating cellular morphogenesis in eukaryotes, the downstream

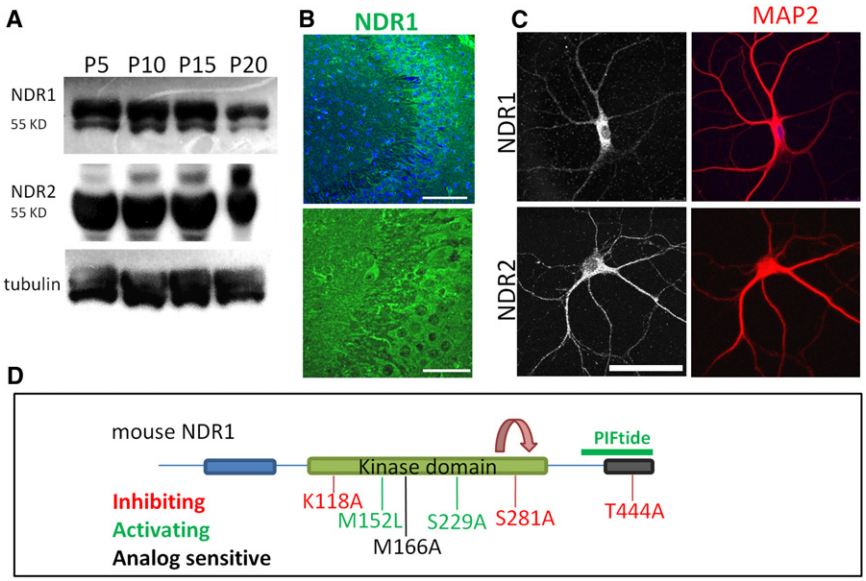

E

Mutant name	Site	Kinase activity
NDR1-AA	S281A & T444A	Inactive
NDR1-KD	K118A	Kinase dead
NDR1-CA	C-terminal hydrophobic motif is replaced with PRK2 hydrophobic motif (PIFtide)	Constitutively active
NDR1-as	M166A, M152L & S229A	Analog sensitive & rescued activity
NDR1-as-CA	M166A, M152L & S229A, (PIFtide)	Analog sensitive & rescued activity Constitutively active

Figure 1. Expression of NDR1, NDR2, and Autophosphorylated NDR1/2 Proteins in Neurons

(A) NDR1 and NDR2 proteins are present in the brain during development. Western blots of mouse brain lysates from postnatal day (P)5, P10, P15, and P20 probed by a mouse monoclonal antibody raised against NDR1 and an NDR2-specific polyclonal antibody we raised for this study. Antitubulin blot is shown as loading control.

(B) (Top) Immunostaining with NDR1 antibody (green) shows endogeneous NDR1 in CA3 pyramidal cell layer (nuclei are labeled with DAPI shown in blue). Scale bar is 100 μm. (Bottom) Immunnostaining with NDR1 antibody (green) labels dendrites and cytoplasm in CA3 hippocampus. Scale bar is 50 μm.

(C) Cultured hippocampal neurons stained against NDR1 or NDR2 antibodies described above costained with MAP2 (microtubule associated protein 2, a dendritic marker) showing NDR1 and NDR2 in dendrites and cytoplasm. Scale bar is 50 μm.

(D and E) NDR1 mutations used in this study. Red is loss of function, green is gain/rescue of function, and black is analog-sensitive mutants. See also Figure S1.

phosphorylation targets of NDR1/2 remain largely unknown, except for two substrates for the NDR1/2 yeast homolog Cbk1: Sec2p (Kurischko et al., 2008) and Ssd1p, a nonconserved protein (Jansen et al., 2009), and a recently identified NDR1/2 substrate p21 (Cornils et al., 2011). To elucidate the mechanism of NDR1/2 kinase actions in neurons, it is important to identify the direct phosphorylation targets of NDR1/2 and their functions in the brain.

In this study, we investigated NDR1/2 function in cultured rat hippocampal neurons and in mouse cortical neurons in vivo by perturbing its function via the expression of dominant negative and constitutively active NDR1/2 and siRNA. We found that NDR1/2 kinases limit dendrite branching and length in cultures and in vivo, analogous to the roles of their fly homolog Trc. Additionally, NDR1/2 kinases were also required for mushroom spine synapse formation as NDR1/2 loss of function led to more immature spines, both in cultures and in vivo, as well as a reduction in the frequency of miniature excitatory postsynaptic currents (mEPSCs) in neuronal cultures. To uncover the direct targets of NDR1/2, which control dendrite branching and mushroom spine formation, we used chemical genetics to create a mutant NDR1 capable of uniquely utilizing an ATP analog not recognized by endogeneous protein kinases (Blethrow et al., 2008; Shah et al., 1997). An advantage of this method is that it identifies not only the substrates but also the phosphorylation sites. We identified five potential NDR1 substrates in the mouse brain and chose two for functional validation. We show that one NDR1 substrate is another kinase, AP-2 associated kinase-1 (AAK1), which regulates dendritic branching as a result of NDR1 phosphorylation. Another substrate is the Rab8 guanine nucleotide exchange factor (GEF) Rabin8 (a Sec2p homolog), which we find is involved in spine synapse formation. These studies uncover two downstream signaling pathways defined by a kinase (AAK1) and a GEF (Rabin8), which regulate complex neuronal dendritic and synaptic phenotypes orchestrated by NDR1/2.

RESULTS

NDR1 and NDR2 Are Expressed in the Brain during Development

NDR1 and NDR2 transcripts have been found in the brain by reverse transcription polymerase chain reaction (RT-PCR) and northern blot (Devroe et al., 2004; Stegert et al., 2004), and NDR2 mRNA has been localized via in situ hybridization in various brain regions, including the hippocampus and cortex (Stork et al., 2004). To determine the developmental profile of NDR1 and NDR2 expression, we probed brain lysates from postnatal day (P)5, P10, P15 and P20 via a mouse monoclonal antibody raised against NDR1 and a polyclonal antibody we generated that is specific for NDR2 (see Experimental Procedures). Both antibodies recognized a major protein band, which was present throughout development, at ~55 KD (Figures 1A;

Figure S1A available online). The NDR1 antibody did not recognize overexpressed NDR2, and the NDR2 antibody did not recognize overexpressed NDR1 in COS-7 cells, demonstrating their specificity (Figure S1B).

Immunocytochemistry using these antibodies revealed that NDR1 and NDR2 are present in the cytoplasm in hippocampal pyramidal neurons and in the cortex (Figure 1B and data not shown) and are found throughout the cell body and dendrites in dissociated hippocampal neurons in culture (Figure 1C). NDR1 was also present in the nucleus in agreement with previous reports (Millward et al., 1999; data not shown).

NDR1/2 Are Necessary and Sufficient to Limit Dendrite Branching and Total Length

In order to investigate NDR1/2′s cell autonomous function in dendrite development, we used three approaches. Dominant-negative or constitutively active NDR1/2 expression, siRNA knockdown of NDR1 and NDR2, and a chemical genetics approach to block NDR1 activity were used. NDR1 mutations used in this study are shown in Figures 1D and 1E. We found similar results with all three approaches.

The biochemical activation mechanism of NDR kinases has been established. MST3 kinase phosphorylates NDR1/2 at its C-terminal hydrophobic residue T444 to activate it (Stegert et al., 2005). NDR1/2 can be activated by okadaic acid (OA) via inhibition of protein phosphatase 2A, facilitating phosphorylation at T444 and the autophosphorylation at S281 (Stegert et al., 2005). MOB1/2 binding to the N-terminal region of NDR kinases is required for the release of auto-inhibition and maximal activity (Bichsel et al., 2004). Autophosphorylation site S281 is critical for NDR1/2 kinase activity. In order to test NDR1/2′s role in dendrite development, we first generated dominant negative and constitutively active NDR1 mutants (Figures 1D and 1E). For dominant negative NDR1, we mutated Ser281 and Thr444 to Alanine (S281A; T444A, NDR1-AA) or catalytic lysine to alanine (K118A, NDR1-KD); both mutants have no kinase activity (Millward et al., 1999; Stegert et al., 2004). To obtain constitutively active NDR1, we replaced the C-terminal hydrophobic domain with that of PRK2 (PIFtide), similar to the generation of constitutively active NDR2 (Stegert et al., 2004).

Kinase activity levels of NDR1 kinase dead (NDR1-KD) and constitutively active (NDR1-CA) mutants were confirmed by in vitro kinase assay with immunoprecipitated NDR1 using an NDR1 substrate peptide as the kinase target (Stegert et al., 2005; Figure S4A). We then expressed mutant NDR1 proteins together with GFP to test for their effect on the morphology of cultured hippocampal neurons. Neurons were transfected at DIV6-8 to perturb NDR1/2 function during dendrite development and analyzed at DIV16. With low transfection efficiency, it was possible to investigate the cell-autonomous function of NDR1/2 (Figure 2A). We found that NDR1-KD resulted in increased proximal dendrite branching, whereas NDR1-CA caused a major reduction in proximal dendritic branching (Figures 2A and 2B). Total dendrite branch points were also increased in NDR1-AA and NDR1-KD and reduced in NDR1-CA (Figure 2D). In addition, NDR1-CA resulted in a larger number of branch crossings at 340 μm in Sholl analysis (Figure 2B), indicating that NDR1 activity may produce longer main dendrites at the expense of proximal dendrite branches. Total dendrite length was increased with NDR1-KD, and the reduction with NDR1-CA was nearly significant ($p = 0.05$; Figure 2F). These results indicate that NDR1 activity inhibits proximal dendrite growth and branching during development. We found that mutant NDR2 expressions in neurons yielded comparable results (data not shown).

To corroborate these findings, we next used NDR1 and NDR2 siRNA to knock down NDR1/2 function. SiRNA sequences were chosen based on knockdown efficiency of overexpressed NDR1 or NDR2 in HEK293 cells (Figure S2A). These siRNAs partially knocked down the endogeneous protein and were compatible with neuronal viability (Figure S7A). We find that the expression of NDR1 and NDR2 siRNA together (but not alone) increased proximal branching, total branch points, and total length (Figures 2A, 2C, 2E, and 2G) as did dominant negative mutants, supporting NDR1/2′s role on inhibiting exuberant growth. This effect was rescued by co-expression of siRNA-resistant NDR1 (NDR1*; Figures 2C, 2E, and 2G) or siRNA-resistant NDR2 (Figures S2F and S2G), indicating that the effect was indeed due to loss of NDR1/2 kinase function. Our data suggests that NDR1 and NDR2 could have redundant functions in dendrite development. However, it is possible that reduction of NDR1 or NDR2 with their respective siRNA does not bring the protein level below a threshold at which neuronal morphology is altered, but cumulative reduction of both leads to the observed defects, and there could be synergistic interaction between NDR1 and NDR2. Taken together with Trc's role on dendrite development of sensory neurons in fly, where *trc* mutants show increased branching and increased total length of dendrites (Emoto et al., 2004), our findings reveal an evolutionarily conserved function of NDR1/2 in dendrite morphogenesis.

We next employed chemical genetics to manipulate NDR1 function in hippocampal cultures. We first mutated the ATP binding pocket gatekeeper Methionine to Alanine (M166A) to make an analog-sensitive NDR1 (NDR1-as), which can use bulky ATP analogs instead of ATP and can be blocked by kinase inhibitors, such as 1-Na-PP1 (Bishop et al., 2000). We further introduced two rescue mutations in the kinase domain (M152L and S229A) to increase kinase activity, because NDR1-M166A had reduced ATP usage (Figures 1D and 1E; Zhang et al., 2005). Although the M166A gatekeeper mutation resulted in reduced ATP-γ-S usage (Figure 5B), M152L and S229A rescue mutations led to the recovery of ATP-γ-S usage albeit at a lower level than Benzyl-ATP-γ-S, as expected, which were blocked by 1-Na-PP1 (Figure S2B). We transfected neurons with activated NDR1-as at DIV8 and investigated the effect of NDR1 on dendrite development with or without 1-Na-PP1 inhibition from DIV8 to DIV16. We found that 1-Na-PP1 inhibition of NDR1-as resulted in increased proximal branching (50 μm), total branch points, and total length (Figures 2A, 2H, 2I, and 2J), likely due to a dominant negative effect. Activated NDR1-as treated with the vehicle DMSO resulted in larger dendrite arbor with a greater number of branch crossings at 340 μm in Sholl analysis (Figures 1A and 1H), likely due to increased NDR1 activity. These results further confirm that NDR1 functions to reduce proximal dendrite branching and NDR1 activity may in turn facilitate dendrite arbor expansion distally.

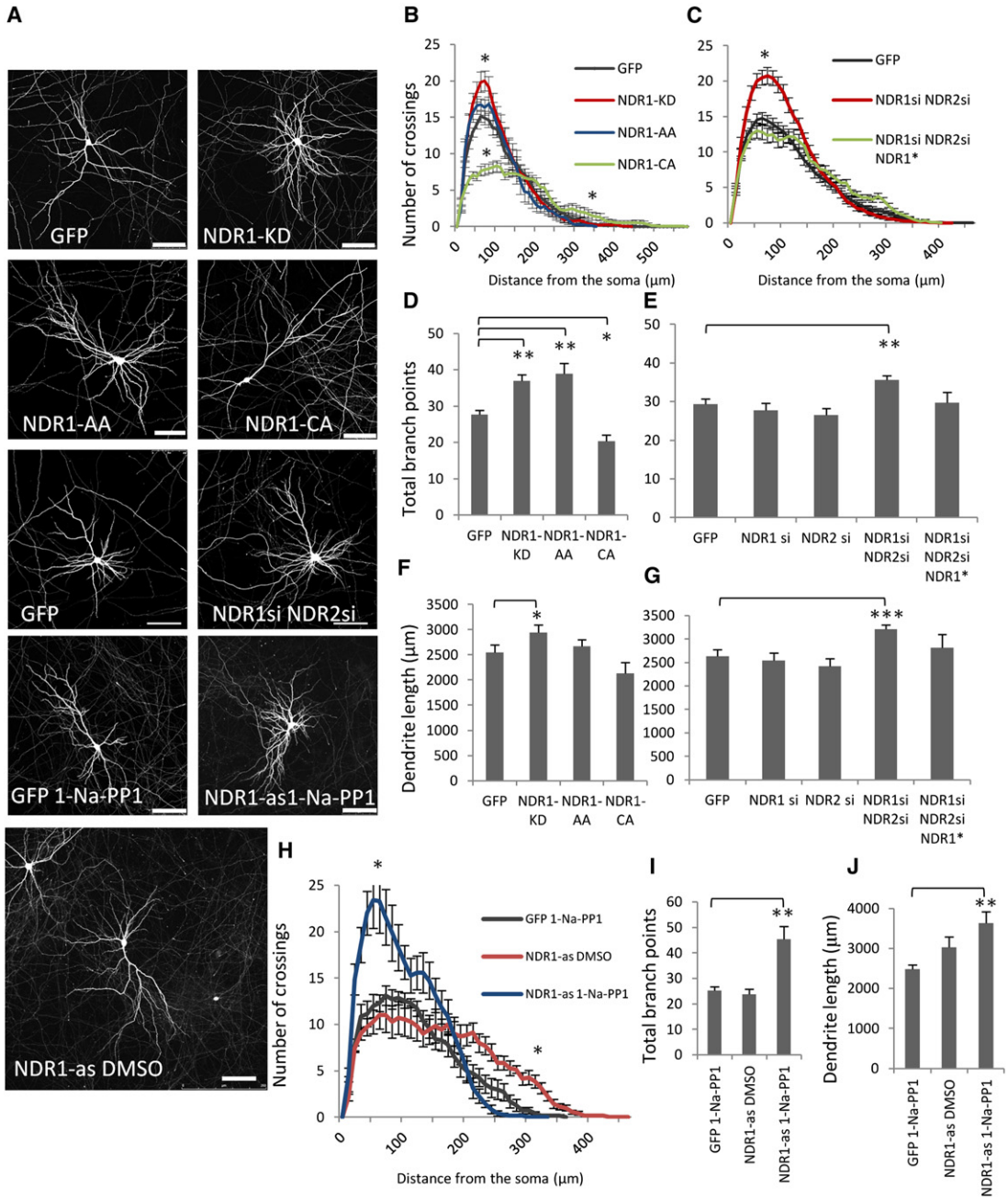

Figure 2. NDR1/2's Role on Dendrite Development

(A) Hippocampal neurons expressing NDR1 mutants or siRNA together with GFP. Scale bars are 100 μm.

(B) Sholl graphs of dendrites of neurons transfected with GFP alone or GFP cotransfected with NDR1 mutants. N of neurons = 21, 16, 18, and 11 for GFP, NDR1-KD, NDR1-AA, and NDR1-CA, respectively.

(C) Sholl graphs of neurons expressing GFP plasmid or GFP plasmid which also expresses siRNA. For dual NDR1 and NDR2 siRNA knockdown, NDR1 siRNA and NDR2 siRNA plasmids were cotransfected. For rescue with siRNA resistant NDR1 (NDR1*), this plasmid was cotransfected with NDR1si and NDR2si. n = 14, 13, and 9 for GFP, NDR1si NDR2si, and NDR1si NDR2si rescue, in order.

(D and E) Total dendrite branch point analysis for NDR1 mutant expression and siRNA experiments, respectively.

(F and G) Total dendrite length analysis for NDR1 mutant and siRNA experiments, respectively. (n = 10 and 10 for NDR1si and NDR2si.)

(H) Sholl analysis for chemical genetics inhibition of analog-sensitive NDR1-as by 1 μM 1-Na-PP1. DMSO (solvent) was used as control. n = 7 for each group.

(I) Total branch points and (J) total length analysis for chemical genetic NDR1-as inhibition experiment. *$p < 0.05$, **$p < 0.01$, and ***$p < 0.001$ in all graphs in all figures assessed by the Kruskal Wallis nonparametric test followed by dual test with Dunn's method in comparison with GFP control (unless otherwise indicated). Error bars are standard error of the mean in all graphs. Stars on Sholl graphs statistical comparisons with Kruskal-Wallis followed by Dunn's method at 50 μm or 340 μm distance from the soma. See also Figure S2.

We then asked if NDR1 function is necessary at earlier ages by transfecting neurons with control plasmid or NDR1-AA at DIV4 and daily performing live imaging until DIV14. We found that at DIV7 and at all later ages NDR1-AA neurons had higher total branch numbers than did the control, indicating that NDR1 function is already required at DIV4-7 (Figure S2C). Next, we asked if increased branching is the result of more branch formation or less branch retraction. Whereas the high cell-to-cell variability rendered it difficult to discern a significant effect in the number of branches formed or lost over a period of 8 hr (Figure S2D), individual neurons expressing NDR1-KD displayed net branch addition, and control neurons showed a net reduction of branches (Figure S2E). NDR1-CA neurons showed no net change of branch numbers over this period (Figure S2E). Therefore, whereas NDR1-KD and NDR1-CA ultimately affect the number of branches, it remains possible that branch formation and/or elimination contribute to the changes in dendrite branching observed in cohort analysis.

NDR1/2 Control Dendritic Spine Development and Excitatory Postsynaptic Function

NDR kinases have important roles in polarized growth; however, their function in synaptic development has not been investigated. We therefore analyzed dendritic spine morphologies in neurons expressing dominant negative or constitutively active NDR1 or siRNA. Dendritic spines can be categorized in accordance with their morphology (Harris, 1999; Yuste and Bonhoeffer, 2004). To evaluate the effect of NDR1/2 on the growth of spines, we divided spines into four categories (Konur and Yuste, 2004). Mushroom spines (MS) are protrusions with a head and a neck; filopodia (F) spines are thin protrusions without a discernable spine head; atypical (A) spines are protrusions with irregular shape; and stubby (St) spines are short protrusions without a discernible spine neck (Figure 3B). Spine morphology is correlated with synaptic function, where mushroom spines contain AMPA receptors in proportion to the size of spine's head, whereas filopodia mostly lack these receptors (Matsuzaki et al., 2001). Spine morphologies are especially diverse during early development (Fiala et al., 1998; Konur and Yuste, 2004). Atypical and stubby protrusions are more common in developing tissue, but dendrites contain mostly mushroom spines, representing mature synapses later in development (Harris, 1999).

We transfected neurons at DIV6-8 and analyzed them at DIV16. Expression of dominant negative NDR1 (NDR1-KD or NDR1-AA) caused a robust increase of filopodia and atypical protrusion densities, together with a reduction in mushroom spine density (Figures 3A–3C), indicating that NDR1 function is necessary for mushroom spine formation. In contrast, NDR1-CA drastically reduced the total dendritic protrusion density as a result of the significant reduction in mushroom, filopodia, and stubby spines (Figures 3A–3C). Although there was variability in the absolute densities of dendritic spine categories among cultures, decreasing or increasing NDR1 activity consistently induced comparable changes as illustrated here. Robust inhibition of dendritic protrusions by NDR1-CA suggests that excessive NDR1 activity reduces all actin-rich dendritic protrusions. Similar to the dominant negative effects of NDR1 mutants, NDR1siRNA + NDR2siRNA also resulted in increased filopodia and atypical protrusions and decreased mushroom spine densities, which was rescued by co-expression of siRNA-resistant NDR1 (NDR1*; Figures 3A and 3D). The difference in the extent of filopodia/atypical protrusion increases between dominant negative mutants and siRNA might be due to incomplete knockdown by siRNAs. In addition, the total numbers of dendritic protrusions were not completely restored by NDR1*, suggesting a small, nonspecific effect of siRNA expression. These data indicate that NDR1/2 are required for efficient formation and/or maturation of mushroom spines. Expression of NDR2-KD and NDR2-CA yielded alterations similar to those induced by the corresponding NDR1 mutants (data not shown).

To determine whether changes in spine morphologies reflected defects in synaptic function, we recorded miniature excitatory postsynaptic currents (mEPSCs) in cultured hippocampal neurons transfected the same way (Figure 3E). We found that mEPSC frequency was reduced by NDR1-KD and by NDR1siRNA + NDR2siRNA, and the effect caused by siRNA knockdown was rescued by siRNA-resistant NDR1, indicating that NDR1/2 are necessary for active synapse formation (Figure 3F). Interestingly, NDR1-CA also caused a reduction in mEPSC frequency indicating that uncontrolled NDR1 activity can also inhibit active synapse formation (Figure 3F). We did not find a difference in mEPSC amplitude (Figure 3G), suggesting that NDR activity affects the number of active synapses rather than the strength of each synapse. Furthermore, coimmunostaining with post- and presynaptic markers indicate that synapses are most often made directly on dendritic shaft in NDR1-CA-expressing neurons in contrast to neurons expressing NDR1-KD or GFP alone (Figure S3A). These observations indicate that mEPSCs in NDR1-CA neurons could originate from synapses on dendritic shafts and support the notion that the reductions in the total number of synapses in NDR1-KD- and NDR1-CA-expressing neurons leads to reduced mEPSC frequency.

Our data revealed that both loss and gain of function of NDR1/2 altered spine morphogenesis. NDR1/2 loss of function reduced mushroom spines and increased filopodia and atypical protrusions. The reduction in mushroom spines is reflected in reduced mEPSC frequency. In contrast, uncontrolled NDR1-CA activity led to retraction of all dendritic protrusions, most likely via a mechanism distinct from the process for mushroom spine formation. The reduction in mushroom spines, along with other dendritic protrusions, is also reflected in reduced mEPSC frequency. Thus, our data indicate that strictly controlled NDR1/2 activity is required for proper dendritic spine development.

NDR1/2 Limit Dendrite Branching and Controls Spine Morphology In Vivo

We next altered NDR1/2 function in layer 2/3 cortical pyramidal neurons in vivo by expression of dominant negative or constitutively active NDR1, as well as siRNA, via in utero electroporation at embryonic day (E)14.5–E15.5. Analysis of labeled layer 2/3 neurons in P18–P20 brains revealed no effect on neuronal migration by NDR1/2 manipulations (data not shown). We measured dendritic arborization within 150 μm from the soma, which included basal dendrites, and proximal region of the

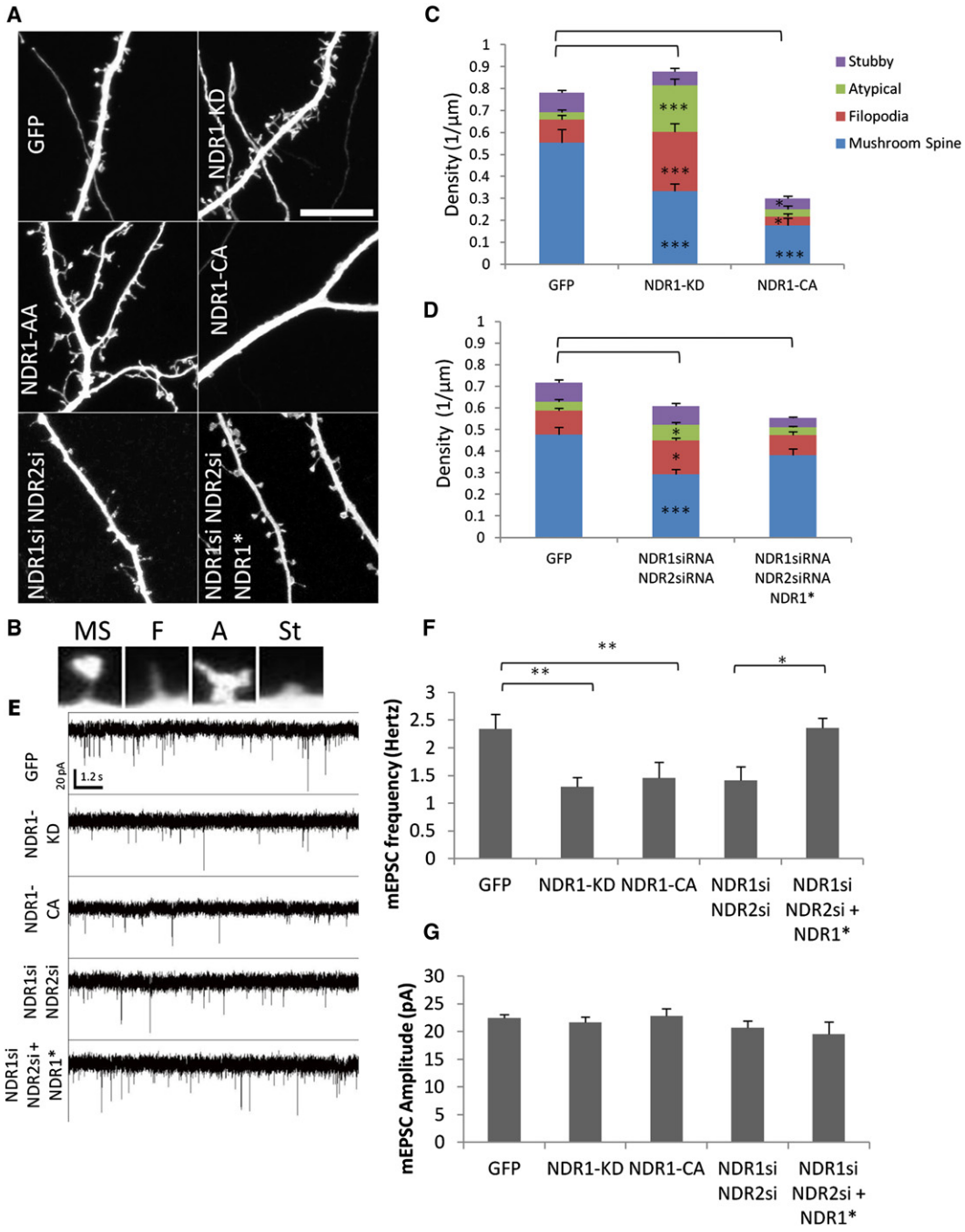

Figure 3. NDR1/2's Role on Dendritic Spine and Excitatory Postsynaptic Development

(A) Dendritic spines of neurons transfected with NDR1 mutants or siRNA are shown; scale bar is 10 μm.

(B) Dendritic spine categories: MS, mushroom spine; F, filopodia; A, aypical; St, stubby.

(C) Effect of NDR1 dominant negative and constitutively active expression on different categories of dendritic spine densities. n of cells = 6, 9, and 8 for each group, in order.

(D) Effects of NDR1 and NDR2 knockdown by siRNA on dendritic spines. n = 12, 16, and7 for each groups, in order.

(E) Examples of whole-cell patch-clamp recordings of mEPSC from transfected hippocampal neurons.

(F) Comparison of frequency and (G) amplitude of mEPSCs. n = 24, 15, 16, 11, and 8 for GFP, NDR1-KD, NDR1-CA, NDR1si NDR2si, and NDR1si NDR2si NDR1* rescue, respectively. NDR1* is wild-type NDR1 cDNA, which lacks the 3′ UTR containing the siRNA target sequence and is therefore siRNA resistant. See also Figure S3.

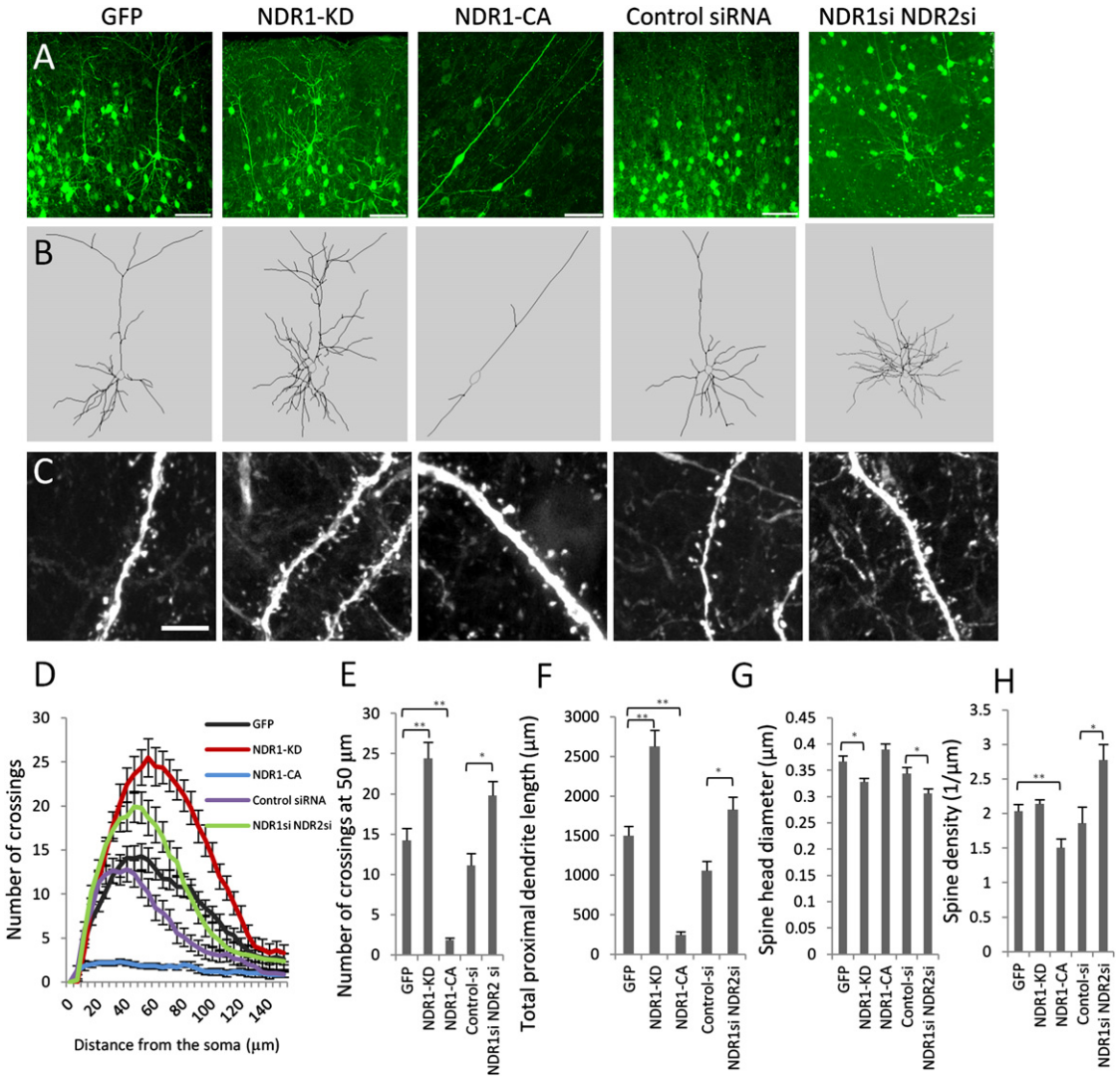

Figure 4. In Vivo Analysis of NDR1 Mutants and siRNA by In Utero Electroporation

(A) Projected z-stacks of GFP and NDR1 mutants or siRNA expressing layer 2/3 neurons are shown. Scale bars are 75 μm, except the NDR1-CA scale bar is 50 μm.

(B) Drawings of neurons in (A).

(C) Representative images of dendritic spines on labeled layer 2/3 pyramidal neuron basal dendrites. Scale bar is 5 μm.

(D) Sholl analysis of dendrites of layer 2/3 neurons. Analysis was done for first 150 μm distance from the soma, focusing on basal dendrites and apical oblique dendrites proximal to the soma. n = 15, 10, 6, 9, and 16 for GFP, NDR1-KD, NDR1-CA, Control siRNA, and NDR1si NDR2si, respectively.

(E) Comparison of dendritic branch crossings via Sholl analysis at 50 μm from the soma.

(F) Total dendrite length comparison between groups, including dendrites 150 μm from the soma.

(G and H) Spine analysis. Spine head diameter (G) and spine density comparison between groups (H). n = 7, 12, 8, 7, and 7 for GFP, NDR1-KD, NDR1-CA, control-si, and NDR1si NDR2si, respectively. See also Figure S3.

apical dendrite. The apical tufts were not included in the analysis, because they were mostly cut away in our sections. We found that NDR1-KD or NDR1siRNA + NDR2siRNA expression (which reduces NDR1 and NDR2, respectively; Figures S3E and S7B) increased dendrite branching at 50 μm from the soma and the total dendrite length, when compared with vector control and control-siRNA, respectively (Figures 4A, 4B, 4D–4F). In contrast, NDR1-CA expression dramatically reduced branching and dendrite length (Figures 4A, 4B, 4D–4F), the reduction in branching was uniformly apparent in all GFP-expressing cells (Figure S3B). NDR1-CA-expressing neurons appeared healthy (Figures S3C and S3D). These results agree well with our findings in hippocampal cultures and show that NDR1/2 function is necessary and sufficient to limit dendrite branching in vivo as well as in vitro.

In perfused brains from animals subjected to in utero electroporation, we did not observe variable dendritic protrusion morphologies at the resolution imaged (Figure 4C). The

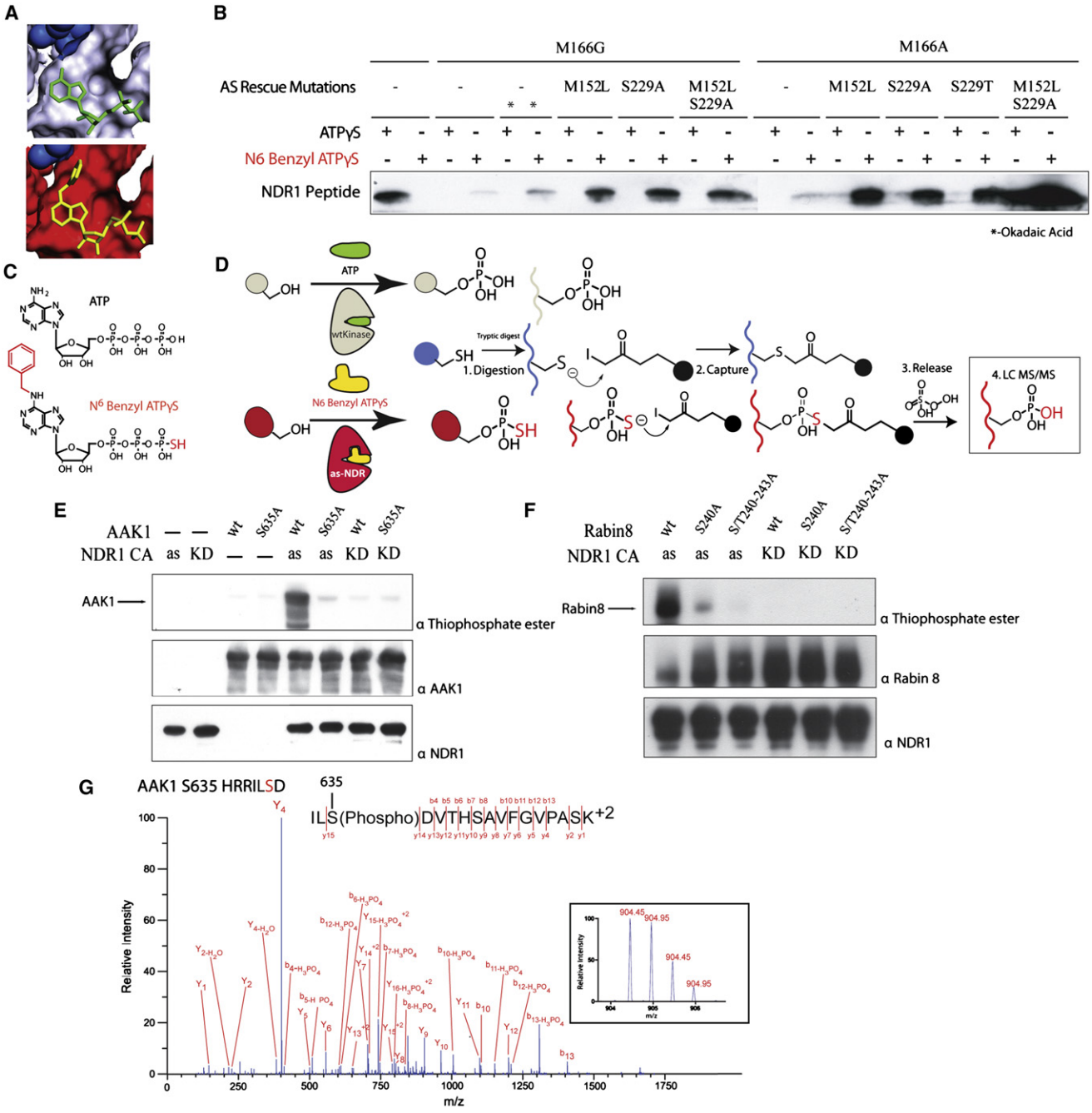

Figure 5. Identification of NDR1's Phosphorylation Targets by Chemical Genetics

(A) Depiction of ATP binding site of wild-type Src kinase with ATP (green; top) and as-Src with Benzyl-ATP-γ-S (yellow; bottom). Mutation in gatekeeper residue (blue) resulted in an affinity pocket, where bulky ATP analog binds.

(B) NDR1-as mutants (M166A and M166G) in NDR1-CA use Benzyl-ATP-γ-S, and their efficiency is increased by two-point mutations in the kinase domain M152L and S229A/T. HA-tagged kinase was expressed and purified from COS-7 cells using HA tag. Kinase reaction was done using NDR substrate peptide. Thiophosphorylation was detected by antithiophosphate ester antibody.

(C) Structures of ATP and Benzyl-ATP-γ-S are shown.

(D) Covalent capture method for kinase substrate identification. A protein phosphorylated by endogeneous kinases is depicted in gray. A protein thiophosphorylated by NDR1-as is depicted in red. Blue depicts a protein that contains a Cysteine.

(E and F) Validation of AAK1 and Rabin8 phosphorylation sites by direct in vitro kinase assays. (E) Confirmation of AAK1 S635 as the NDR1-specific phosphorylation site. In vitro kinase assays were performed by incubating the indicated NDR1-as-CA with purified wild-type AAK1-HA or S635A AAK1-HA protein. Reaction was done using Benzyl-ATP-γ-S, which is used by NDR1-as-CA and not AAK1 to prevent the phosphorylation signal caused by AAK1 autophosphorylation when regular ATP is used. Immunoblot with antithiophosphate ester-specific antibody reveals S635 on AAK1 as the only NDR1

predominant protrusion type observed in vivo was mushroom spine. Therefore, we measured spine head diameters and spine density as the functional parameters of these postsynaptic structures. We found that NDR1-KD and NDR1siRNA + NDR2siRNA decreased dendritic spine head diameter (Figure 4G), suggesting that NDR1/2 is required for dendritic spine development in vivo. These results are in agreement with our hippocampal culture results, in which NDR1/2 promoted mushroom spines and active synapses and limited immature protrusions. It is possible that certain factors that contribute to spine formation and stabilization, which are present in vivo, are largely absent in cultures. Such differences between cultures and in vivo studies, caused by similar manipulations of NDR1/2 activity, might result in the different spine phenotypes we observe (Figures 3A–3D and 4G).

We also found that dendritic spine density was reduced in NDR1-CA-expressing neurons and was increased by NDR1siRNA + NDR2siRNA in vivo, while we did not observe a significant change with NDR1-KD (Figure 4H). It is possible that the NDR1-KD expression level was not sufficient to cause increased spine density in vivo. NDR1/2 participates in limiting dendritic spine density as is demonstrated in cultured NDR1-CA-expressing neurons (Figures 3A–3D). Our data supports that NDR1 activity is necessary in limiting dendritic spine numbers in vivo as well.

Overall, our data shows that NDR1/2 regulates spine morphology by enlarging spine heads and limiting spine numbers in vivo. These data, together with data from neuronal cultures (Figure 3), support a role for NDR1/2 function in dendritic spine morphogenesis.

Chemical Genetic Identification of NDR1 Kinase Substrates Reveal Multiple Targets in Vesicle Trafficking

Having found NDR1/2 function important for dendrite arborization and synaptic development, we next looked into the underlying mechanisms. Since there were no known substrates of NDR1/2, we utilized the chemical genetic substrate labeling method followed by phospho-specific covalent capture (Blethrow et al., 2008) to identify NDR1 substrates. This method utilizes analog-sensitive kinases, in which the hydrophobic gatekeeper residue is replaced by a smaller amino acid, to allow binding and utilization of ATP analogs modified with bulky substitutions. The crystal structure of the Src ATP binding pocket in analog-sensitive mutants depicts how larger ATP analogs (Figure 5C) can fit the binding pocket of Src-as (Figure 5A).

We generated two analog-sensitive NDR1-CAs (M166A and M166G). In order to identify which bulky ATP-γ-S analog is most compatible with the mutant kinase, we performed an in vitro kinase reaction with these mutants using NDR1's target peptide as described previously (Stegert et al., 2005). The thiophosphorylated substrate is detected by antithiophosphate ester antibody on a western blot after esterification by para-nitro benzyl mesylate (PNBM; Allen et al., 2007). We found that NDR1-CA M166A used Benzyl-ATP-γ-S; however, the ATP analog usage was reduced (Figure S4B). To rescue NDR1 kinase activity we, mutated two residues known to be suppressor mutations that can rescue kinase activity when the gatekeeper residue is mutated (Zhang et al., 2005) and obtained NDR1-as-CA with increased kinase activity (NDR1-CA with M166A, M152L, and S229A mutations; Figures 1D, 1E, and 5B). We used this kinase (NDR1-as-CA) in subsequent substrate identification experiments. To perform labeling reactions in which NDR1-as-CA would thiophosphorylate substrates with Benzyl-ATP-γ-S, we reacted 10 μg of purified kinase with 1 mg brain lysate protein. Labeled lysate was treated by covalent capture for substrate identification (Blethrow et al., 2008; Hertz et al., 2010). Briefly, labeled protein lysate is digested by trypsin and then thiol-containing peptides (including thiophosphorylated substrates and cysteine-containing peptides) are captured by thiol reactive resin, whereas non-thiol-containing peptides are washed away. In the third step, beads are treated with Oxone to oxidize sulfur and elute phosphopeptides by spontaneous hydrolysis of thiophosphate linkage, whereas cysteine-containing peptides remain attached to the beads by thioether bonds. Finally, the eluted peptides are analyzed by liquid chromatography/tandem mass spectrometry to identify not only the substrates but also the phosphorylation sites, which is a major advantage of the method (Figure 5D).

In each experiment, we included two negative controls (lysate alone and lysate reacted with NDR1-KD) in parallel; with these controls we could disregard abundant proteins that are detected nonspecifically. We have carried out substrate labeling from brain lysates eight times, using P3 (2X), P8 (5X), and P13 (1X) brains, to identify potential NDR1 targets. We identified five phospho-proteins that are specific to NDR1-as-CA and are detected in more than one experiment (Table 1). Strikingly, four of these contained the consensus sequence of HXRXXS/T, which is highly similar to the one reported for the NDR1 homolog Cbk1p (HXRRXS/T; Mazanka et al., 2008; Table 1). The remaining candidate was not included in the table, because the phosphorylation site was preceded by acidic amino acids, rendering it an unlikely NDR1 substrate. In addition, we cultured dissociated cortical neurons on transwell insert culture dishes in order to harvest neuronal processes but not cell bodies to simplify total protein content. We identified one additional candidate with the same consensus site: Rab11fip5 (Rab11 family interacting protein 5; Table 1). Proteins without the consensus sequence were not included in the table for this experiment.

Thus, we have identified five putative NDR1 substrates: AAK1 (AP-2 associated kinase 1) and Rabin8 (Rab8-GEF), both of which are known to function in vesicle trafficking (Henderson

phosphorylation site on AAK1. (F) Similar experiment as in (E), demonstrating Rabin8 as an NDR1 phosphorylation substrate protein. Rabin8 is phosphorylated by NDR1-as-CA in vitro, and this phosphorylation is greatly diminished in the Rabin8 S240A mutant, indicating this site as the major phosphorylation site. When S/T 240-243 are all mutated to Ala (Rabin8-AAAA), NDR1-as-CA can no longer phosphorylate Rabin8, indicating that these residues may be also phosphorylated when S240 is mutated to Ala.

(G) Mass spectroscopy identification of AAK1 phosphorylation by HCD (higher energy C-trap dissociation) spectra analysis of AAK-derived peptide containing phosphorylated S635. See also Figure S4 and Table 1.

Table 1. Candidate Direct Phosphorylation Targets of NDR1

NDR1 Substrate	No. of Experiments Detected and Ages	Phosphorylation Site		Cellular Function
AAK1 (AP2-associated kinase 1)	7 (P3, P8, P13)	**HRR**ILS*D	S635	Endocytosis-receptor recycling
Rabin8 (Rab3AIP- Rab3A interacting protein)	3 (P3, P8, P13)	**HTR**NKS*T	S240	Rab8-GEF, vesicle trafficking, and secretory
PI4KB (pik4cb, Phosphatidyl inositol 4 kinase beta)	2 (P3, P8)	**HQR**SKS*D	S277	Membrane lipid composition and trafficking
Panx2 (Pannexin-2)	2 (P8, P13)	**HTR**HFS*L	S514	Large pore channel
Rab11fip5 (Rab11 family interacting protein 5)	1 (DIV10)	**HKR**TYS*D	S307	Recycling endosome

Eight experiments were conducted. Two were conducted at P3, five were conducted at P8, and one was conducted at P13. Second column shows the number of times the candidate is detected with the detected ages. Columns 3 and 4 show the NDR1 phosphorylation sites and the amino acid in the mouse target proteins. Bold letters indicate NDR1 consensus motif; *indicates the phosphorylated amino acids. Column 5 describes the reported cellular functions of these proteins.

and Conner, 2007; Stenmark, 2009), PI4Kbeta (Phosphatidyl inositol 4 kinase beta), which catalyzes the formation of phosphatidyl inositol 4 phosphate that can give rise to other phosphatidyl inositols (De Matteis et al., 2005), Pannexin-2, a large pore ion channel expressed in the brain (MacVicar and Thompson, 2010), and Rab11fip5, which regulates the small GTPase Rab11 involved in membrane recycling (Horgan and McCaffrey, 2009). Given their high sequence homology, especially in the kinase domain, and indistinguishable biochemical properties as so-far tested, taken together with the ability of NDR1 to rescue for NDR1/2 reduction, NDR1 and NDR2 probably have common substrates.

We were particularly interested in the two most prevalent candidates AAK1 and Rabin8, because both function in intracellular vesicle trafficking. AAK1 was identified in seven out of eight experiments, and Rabin8 was identified in three out of eight experiments. Moreover, the yeast Rabin8 homolog Sec2p is phosphorylated by the yeast NDR kinase Cbk1p (Kurischko et al., 2008), indicating that this kinase regulation might be evolutionarily conserved. We confirmed that AAK1 and Rabin8 were indeed phosphorylated by NDR1 by using direct kinase assay (Figures 5E and 5F). We reacted purified NDR1-as-CA with purified substrate proteins using Benzyl-ATP-γ-S and detected phosphorylation by antithiophosphate ester antibody after esterification with PNBM (Figures 5E and 5F), a method that avoids the background caused by AAK1 autophosphorylation when using radioactive ATP for detection. We confirmed that the AAK1 phosphorylation site was indeed S635, as was identified in mass spectrometry (Figure 5G), since S635A mutant was not phosphorylated (Figure 5E). Furthermore, we generated an antibody that targets AAK1 phosphorylated at S635 (anti-AAK1 P-S635). When coexpressed in COS-7 cells, NDR1-CA specifically phosphorylated S635 of AAK1 in intact cells (Figure S5E). However, it should be noted that this antibody did not exclusively stain the endogenous phosphorylated AAK1 by immunocytochemistry (data not shown).

Rabin8 was phosphorylated by NDR1 at S240 (Figure S4D). We also showed that wild-type NDR1 (activated by okadaic acid) and NDR1-CA could phosphorylate Rabin8 at S240 using ATP-γ-S (Figure S4C). However, there are likely other residues that can be phosphorylated, because the S240A mutant could be still phosphorylated albeit at a reduced level (Figure 5F). Interestingly, Rabin8 S240 was followed by a stretch of T241, S242, and S243. When all S/T240- 243 were mutated to Ala, NDR1 no longer phosphorylated Rabin8 (Figure 5F).

AAK1 Controls Dendrite Arborization in a Similar Way to NDR1/2

Next, we investigated the function of AAK1 on dendrite and spine development. In cultured hippocampal neurons, AAK1 is in the cytoplasm, dendrites, and axons but is excluded from the nucleus as shown by immunostaining of endogeneous AAK1 by the anti-AAK1 antibody (Figure S5C). To test if AAK1 kinase activity depends on S635 in the C-terminal AP-2 binding domain, we examined AAK1 autophosphorylation and found it was not affected by S635A mutation (Figure S5D). To test AAK1's functional role, we expressed AAK1 kinase-dead (AAK1-KD) K74A (Conner and Schmid, 2003), the AAK1 nonphosphorylatable mutant S635A (AAK1-SA) or the AAK1 phospho-mimetic mutant S635D (AAK1-SD), together with GFP in dissociated hippocampal neurons. A small subset of neurons with very high expression of mutant AAK1 looked unhealthy and were not included in the analysis. Similar to the result for NDR1/2 loss of function, AAK1-KD and AAK1-SA had increased branching within 50 μm from the soma (Figures 6A–6C). In contrast, AAK1-SD decreased branching (Figures 6A, 6B–6C) similar to NDR1-CA. Dendrite length was also increased in AAK1-KD and reduced in AAK1-SD mutants (Figure 6D), in a similar way to the effect caused by manipulations of NDR1/2 activity. AAK1 siRNA, which knocked down AAK1 partially (Figures S5A and S7A), increased dendrite branching and length; this effect was rescued with siRNA-resistant AAK1 (Figures 6C and 6D). The dendritic spines appeared normal in AAK1-KD and AAK1-SA mutants; however, neurons expressing AAK1-SD at high levels showed a reduction in dendritic spine density (Figures S5F and S5G). Thus, although overactive NDR1 and AAK1-SD could lead to the elimination of dendritic spines, most likely other NDR1/2 substrate(s) contribute to mushroom spine formation by NDR1/2.

To explore if AAK1 is downstream of NDR1/2 in dendrite development, we performed epistasis experiments. Total plasmid DNA concentration was kept constant between conditions. Control neurons were transfected with GFP expressing empty siRNA plasmid (pGmir), together with HA expressing empty plasmid (prk5). To observe the effect of NDR1/2 loss of

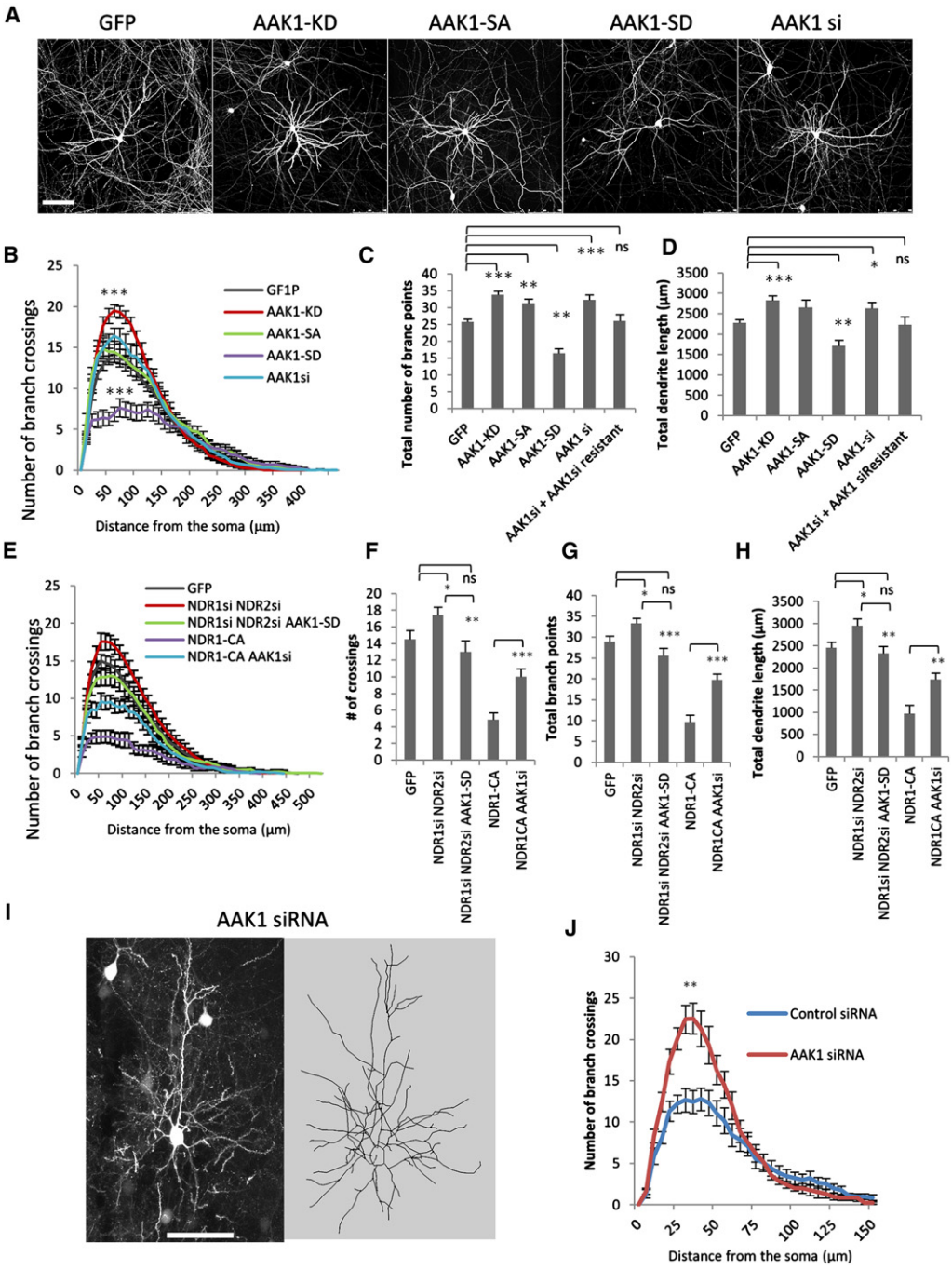

Figure 6. AAK1 Affects Dendrite Branching and Length in Dissociated Hippocampal Neurons

(A) Neurons expressing GFP alone, GFP plus AAK1 mutants (AAK1-KD, AAK1-SA, or AAK1-SD), and AAK1siRNA. Scale bar is 100 μm.

(B) Dendrite branching statistics are done via Sholl analysis at 50 μm distance from the soma. n = 27, 24, 17, 14, 23, and 13 for GFP, AAK1-KD, AAK1-SA, AAK1-SD and AAK1-si, and AAK1si + AAK1 siResistant, respectively.

(C) Total number of dendrite branches and (D). Total dendrite length comparisons.

(E–H) Experiments showing epistasis between NDR1 and AAK1 in hippocampal neurons. Neurons were transfected with GFP + HA, NDR1si NDR2si +HA, NDR1si NDR2si + AAK1-SD-HA, NDR1-CA-myc + GFP, and NDR1-CA-myc + AAK1si (n = 32, 31, 29, 13, and 16, respectively) to test epistasis. (E) Sholl analysis of dendrites. (F) Number of branch crossings at a 40 μm distance from the soma for Sholl analysis in (E). (G) Total number of branch points and (H) total dendrite length of all neurons are shown.

(I and J) In utero electroporation of AAK1 siRNA leads to increased proximal branching. (I) A layer 2/3 neuron expressing AAK1 siRNA, and its drawing is shown. (J) Sholl analysis of AAK1 siRNA-expressing neurons in comparison to Control siRNA. Dendrite branching is increased at 40 μm (n = 9 for each group, $^{**}p < 0.01$). See also Figure S5.

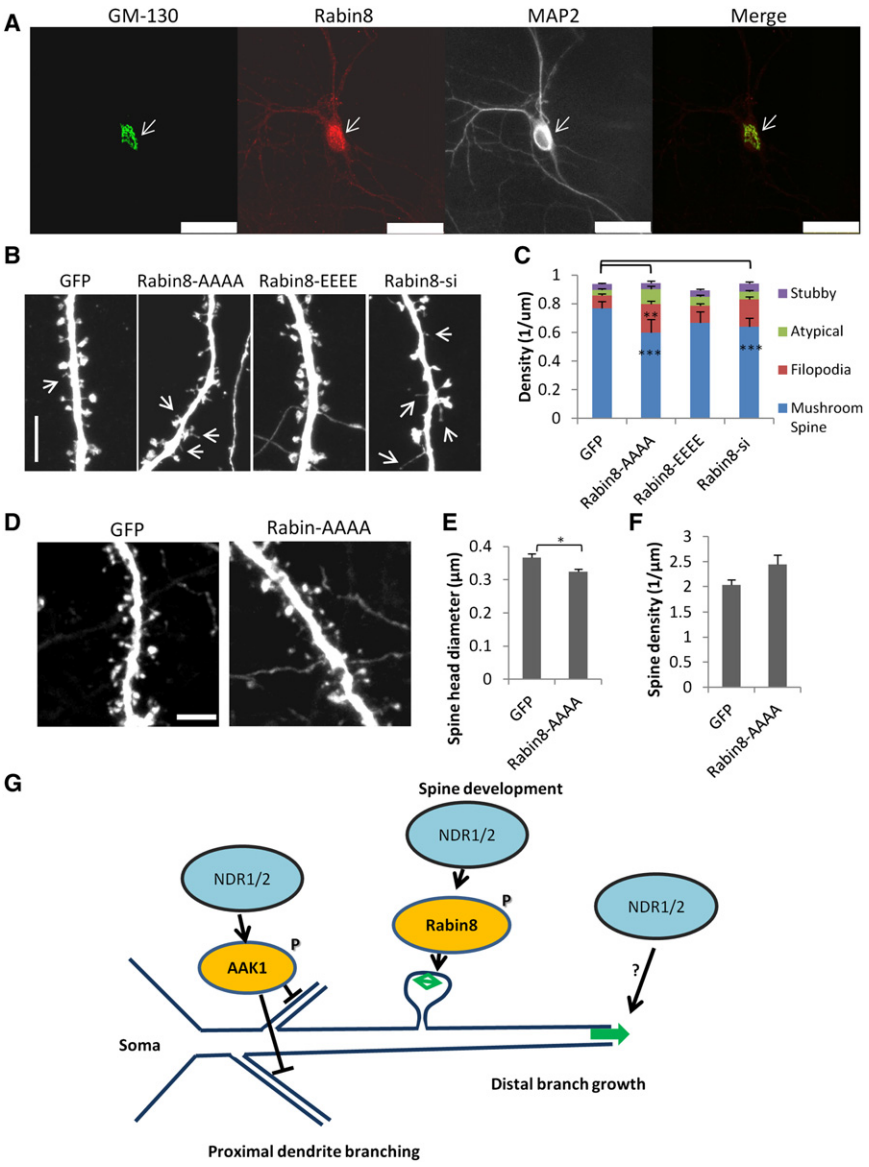

Figure 7. Rabin8 Affects Spine Morphogenesis in Dissociated Hippocampal Neurons

(A) Endogenous Rabin8 immunostaining in cultured hippocampal neurons at DIV10. Perinuclear Rabin8 (red) colocalizes with Golgi marker GM-130 (green). MAP2 depicts dendrites. Scale bar is 25 μM.

(B) Dendritic spine morphologies of control, Rabin8 mutants, and Rabin8 siRNA-expressing neurons. Arrows point to filopodia. Scale bar is 6 μm.

(C) Quantification of spine morphologies. n = 23, 13, 12, and 17 for GFP, Rabin8-AAAA, Rabin8-EEEE, and Rabin8-si, respectively.

(D) In utero electroporation analysis of Rabin-AAAA coexpressed with GFP. Scale bar is 3 μm.

(E) Spine head diameter and (F) spine density analysis are shown for Rabin-AAAA-expressing neurons in comparison to GFP alone (N = 7 and 11 for GFP and Rabin-AAAA, respectively, *p < 0.05).

(G) Summary depicting NDR1/2's function on dendrite development and spine morphogenesis via two of its phosphorylation targets. See also Figure S6.

function, we transfected NDR1siRNA and NDR2siRNA together with equal amounts of empty prk5 vector. This treatment caused an increase in proximal dendrite branching (Figures 6E and 6F), total dendrite branching (Figure 6G), and length (Figure 6H) as was expected. In order to test epistasis, NDR1siRNA and NDR2siRNA were co-transfected with the AAK1-SD-HA construct in prk5 vector. This treatment led to the rescue of dendrite phenotypes induced by NDR1siRNA + NDR2siRNA (Figures 6E–6H). In complementary experiments, we transfected NDR1-CA with GFP expressing empty siRNA plasmid and observed robust reduction in proximal dendrite branching (Figures 6E and 6F), total dendrite branching (Figure 6G), and length (Figure 6H). The reduction in dendrite branching and length with NDR1-CA was more pronounced than in previous results because of the higher plasmid concentration used here. These effects of NDR1-CA were partially rescued with co-expression of AAK1siRNA (instead of empty siRNA plasmid), indicating that AAK1 activity was necessary to limit dendrite branching. These experiments indicate that AAK1 is downstream of NDR1 for limiting dendrite branching.

Finally, in order to further explore the role of AAK1 in vivo we used siRNA knockdown of AAK1 by expressing an AAK1 siRNA in pSuper vector (Figures S5B and S7B). We find that, similar to the results with cultured neurons, AAK1 siRNA increased proximal branching in vivo (Figures 6I and 6J).

Rabin8 Contributes to Spine Development

Next, we investigated Rabin8's function on dendrite development and spine maturation in hippocampal cultures. Immunostaining of endogeneous Rabin8 by anti-Rabin8 antibody showed that Rabin8 is enriched in the Golgi (colocalized with Golgi marker GM-130; Figure 7A), in agreement with the role of Rab8 in post-Golgi trafficking. We first examined its function by mutating the Rabin8 phosphorylation site and expressing these mutants in dissociated hippocampal neurons. We made the Rabin8 phospho mutant, where S240 as well as T241, S242, and S243 were mutated to Alanine (Rabin8-AAAA), which cannot be phosphorylated (Figure 5F), or to Glutamate (Rabin8-EEEE) as a putative phosphomimetic mutant. We found that these Rabin8 mutants and Rabin8 siRNA (Figures S6A and S7A) did not affect dendrite branching (Figures S6C–S6F), indicating that Rabin8 phosphorylation by NDR1 is likely not involved in limiting dendrite branching. The total dendrite length was reduced by Rabin8-AAAA but not Rabin8 siRNA (Figure S6F).

Given that Rabin8 siRNA may not have sufficiently knocked down the Rabin8 level, these observations indicate that Rabin8 is involved in dendrite growth.

Next, we found that the expression of Rabin8-AAAA but not Rabin8-EEEE resulted in increased filopodia and atypical spines, and Rabin8 siRNA increased filopodia density (Figures 7B and 7C). An increase in filopodia was accompanied by a reduction in mushroom spine density by Rabin-AAAA, a trend that was close to reaching significance ($p = 0.07$). These data indicate that Rabin8 phosphorylation by NDR1/2 contributes to spine development by reducing filopodia and increasing mushroom spines. Rabin8-AAAA and Rabin8 siRNA produce less pronounced defects on spines than does NDR1/2 loss of function, possibly because other NDR1/2 substrates act in parallel to Rabin8 and contribute to spine morphogenesis. Alternatively, it is possible that these manipulations do not completely block Rabin8 function because of their incomplete knockdown or dominant negative effect. Given that Rabin-EEEE did not alter spine or dendrite development, this mutant construct may not be able to mimic phosphorylated Rabin8, a notion reinforced by our failed attempt to rescue NDR1siRNA + NDR2siRNA's effect on spine development with Rabin8-EEEE (Figure S6B).

Since Rabin8 is involved in spine maturation, we wanted to learn if it is present in spines with synapses. With immunostaining of postsynaptic marker PSD95 and endogenous Rabin8, we observe Rabin8 in the perinuclear region resembling Golgi and inside the proximal dendrites in neurons (Figure S6G). We cannot rule out the presence of Rabin8 in spines; however, the majority of Rabin8 is found in Golgi. (Figure S6G). NDR1/2 kinases are found throughout the neurites with no particular enrichment in spines (Figures 1B and 1C). Therefore, we hypothesize that NDR1/2 and Rabin8 function in Golgi and dendrites to influence dendritic spine morphogenesis.

Next, we examined Rabin8's role in vivo by expressing Rabin8-AAAA via in utero electroporation (Figures 7D–7F). We found that Rabin8-AAAA reduced spine head diameter similar to the NDR1/2 loss of function effects in vivo. These results further support a role for Rabin8 in formation of mature dendritic spines and implicate a requirement of NDR1/2 phosphorylation in this process.

DISCUSSION

In this study we used dominant negative or constitutively active mutant kinase constructs, and also siRNA expression and chemical genetics to inhibit kinase function, to demonstrate the role of NDR1/2 on proper dendrite arbor morphogenesis and spine growth in mammalian pyramidal neurons in vitro and in vivo (Figure 7G). Using chemical genetic substrate identification by tandem mass spectrometry, we identified several direct substrates of NDR1 and the NDR1 phosphorylation sites. Among these, we validated AAK1 and Rabin8 as NDR1 targets in vitro, and we further showed that AAK1 and Rabin8 are involved in limiting dendrite branching and length and promoting mushroom spine growth, respectively. Dendrite and spine phenotypes induced by the reduction of NDR1/2 function are reminiscent of what has been observed in certain neurodevelopmental diseases, raising the question of whether this signaling pathway may be involved in some neurological disorders (Penzes et al., 2011; Ramocki and Zoghbi, 2008).

Dendrite Pruning and Tumor Suppressors

Proapoptotic signaling cascades can positively regulate dendrite pruning during *Drosophila* metamorphosis (Kuo et al., 2006; Williams et al., 2006) and can also act to weaken synapses in mammals (Li et al., 2010). Since NDR1/2 is also a tumor suppressor (Cornils et al., 2010) and NDR1/2 promotes apoptosis in response to apoptotic stimuli in mammalian cells (Vichalkovski et al., 2008), NDR1/2 adds to the growing list of tumor suppressors that also function in neuronal growth and plasticity. In support of this scenario, the NDR1/2 homolog Trc, which functions in controlling cell size and is implicated in cancer (Koike-Kumagai et al., 2009), is shown to be downstream of TORC2 (target of rapamycin complex 2) in fly.

AAK1 Phosphorylation Regulates Dendrite Branching and Length

Our findings indicate that AAK1 phosphorylation by NDR1/2 mediates, at least in part, its function in limiting proximal dendrite branching. AAK1 is originally identified as an alpha-adaptin binding protein (Conner and Schmid, 2002). It is necessary for efficient endocytosis and receptor recycling in mammalian cells in culture (Henderson and Conner, 2007). AAK1 phosphorylates AP-1 coat component μ1 with similar efficiency as it phosphorylates AP-2 component μ2 (Henderson and Conner, 2007), raising the possibility that it can function in multiple adaptor coat complexes. Adaptor coat complexes are central to vesicle formation on Golgi, endosomes, and the plasma membrane. AP-2 is important for clathrin-mediated endocytosis at the plasma membrane, whereas AP-1 coat is involved in post-Golgi and endosomal vesicle formation (Robinson, 2004). AAK1's yeast homologs Prk1p/Ark1p are also necessary for endocytosis (Sekiya-Kawasaki et al., 2003). Importantly, a potential Cbk1p phosphorylation site is present in Prk1p. Prk1p's role on endocytosis depends on its ability to destabilize actin cytoskeleton at endocytic zones (Toshima et al., 2005). A similar mechanism of actin destabilization could underlie the loss of dendritic spines in NDR1-CA or AAK1-SD-expressing hippocampal neurons. Thus, several lines of evidence suggest that AAK1 regulates intracellular vesicle trafficking. How AAK1 function regulates dendrite morphogenesis remains to be investigated. Intriguingly, AAK1 was recently implicated in regulating various signaling pathways, including Notch (Gupta-Rossi et al., 2011), ErbB4 (Kuai et al., 2011), and *Drosophila* Neuroglian (Yang et al., 2011).

Rab8 GEF Rabin8 Regulates Spine Morphogenesis

Rabin8, first identified as a Rab3-interacting protein (Brondyk et al., 1995), is known to act as a guanine exchange factor for Rab8 rather than Rab3 (Hattula et al., 2002). Rab8 is a small GTPase specialized in post-Golgi vesicle budding and plasma membrane transport (Stenmark, 2009). In hippocampal cultures, we find that Rabin8 is predominantly enriched in the Golgi in soma and proximal dendrites. In yeast, Rabin8 homolog Sec2p was found to be phosphorylated by the yeast NDR1 Cbk1p and was shown to account for a subset of the Cbk1p mutant defects (Kurischko et al., 2008). Importantly, the phosphorylation

site is conserved between Sec2p and Rabin8. It thus appears that the NDR kinase regulation of vesicle trafficking is an evolutionarily conserved function for controlling polarization and cell morphology. Our data suggest that Rabin8, and its phosphorylation by NDR1/2, is involved in mushroom spine development, in cultured neurons, and in vivo. Rabin8 could affect Rab8 function to form and/or deliver post-Golgi vesicles to dendritic membrane contributing to synapse development and increase in spine head diameter. In support of this hypothesis, Rab8 GTPase dominant negative mutant expression in cultured hippocampal slices alters AMPA receptor delivery to surface (Brown et al., 2007; Gerges et al., 2004). Reducing Rabin8 activity causes a spine phenotype milder than that caused by reducing NDR1/2 activity, indicating that other NDR1/2 substrates likely contribute to spine morphogenesis.

NDR1/2 Regulates Dendrite Growth

Loss of NDR1/2 affects preferentially the proximal dendritic branching, causing an increase in proximal branching and a decrease in distal branching. At the same time, NDR1-CA and activated NDR1-as cause increased dendrite branching in the distal regions as is shown in Sholl analysis. Therefore, NDR1/2 may function in promoting distal growth at the expense of proximal branch additions. NDR1/2′s role on branch extension and its potential downstream effectors remain to be investigated. Our data showing reduced dendrite length by Rabin8-AAAA suggests that Rabin8 may be involved in this process. It is important to note that secretory membrane trafficking has been found to be critical for dendrite morphogenesis (Horton et al., 2005; Ye et al., 2007).

Other Candidate Substrates of NDR1/2

The additional potential substrates of NDR1/2 identified in our study could also affect vesicle trafficking. For instance, PI4KB can catalyze formation of phosphatidyl inositol 4 phosphate (PI4P), which is an intermediate in the formation of phosphorylated lipids, such as PI3,4 bisphosphate, PI4,5 bisphosphate, and PI3,4,5 trisphosphate (De Matteis et al., 2005). These phospholipids are known to affect membrane trafficking in post-Golgi and recycling membrane compartments (De Matteis et al., 2005). Another potential substrate, Rab11fip5, is a member of Rab11 family interacting proteins (Horgan and McCaffrey, 2009), which could affect membrane trafficking from recycling endosomes in dendrites (Wang et al., 2008).

Chemical Genetics for Kinase Substrate Identification

The chemical genetics and covalent capture method for kinase substrate identification is a powerful method for mapping of kinase signaling pathways with the unique advantage of phosphorylation site identification (Hertz et al., 2010; Blethrow et al., 2008). This method also allows the identification of substrates from complex tissue homogenates, where the protein complexes may be better preserved in their natural state when compared to other methods that involve gel electrophoresis or protein arrays. We were able to identify five mammalian candidate substrates and validated two of these functionally. Our screen identified the mammalian homolog of one of the yeast substrates Sec2p, confirming its effectiveness and establishing an evolutionarily conserved branch of NDR kinase signaling. Our technique offers an unbiased method for identifying kinase substrates from different tissues, developmental stages and pathological conditions. This approach would make it possible to determine how NDR1/2 activity and targets are altered in pathologies, such as neurodevelopmental and neurodegenerative diseases and cancer.

EXPERIMENTAL PROCEDURES

The use and care of rats and mice used in this study follows the guidelines of the UCSF Institutional Animal Care and Use Committee. Detailed Experimental Procedures can be found in the Supplemental Experimental Procedures.

Cell Culture and Transfection

Hippocampal neurons were cultured from E19 Long-Evans rats at 150,000/coverslip and maintained at serum-free B27-containing media. Plasmid transfections were done using Lipofectamine2000 (Invitrogen, Grand Island, NY, USA).

DNA Constructs and siRNA

Prk5 mammalian expression vector was used for mammalian expression of constructs in cultured neurons and in HEK293 cells. Small hairpins were cloned in a modified pGIPZ (Open Biosystems, Lafayette, CO, USA) for hippocampal cultures and pSuper vector for in utero electroporations.

Electrophysiology

mEPSCs were recorded using whole-cell patch-clamping in the presence of 1 μM tetrodotoxin and 50 μM picrotoxin to isolate excitatory minis.

In Utero Electroporation

E14.5–E15.5 mouse embryos were used for in utero electroporations. Pups were perfused at P18–P20; 100 μm brain sections were immunostained with anti-GFP and imaged using confocal microscopy. Dendrite analysis were done using Neurolucida.

Kinase Assays and Covalent Capture for Phosphorylation Target Identification

NDR kinase assays were done as described (Stegert et al., 2005). Covalent capture of thiophosphorylated substrate proteins was performed as described (Hertz et al., 2010) but with some modifications (see Supplemental Experimental Procedures).

SUPPLEMENTAL INFORMATION

Supplemental Information includes seven figures and Supplemental Experimental Procedures and can be found with this article online at doi:10.1016/j.neuron.2012.01.019.

ACKNOWLEDGMENTS

We thank Mark Wessels, Peter Soba, and Hye-Young Lee for technical help and Chao Zhang for the valuable suggestion of kinase activation mutations. We thank Jon Trinidad for advice on phosphoproteomics and David Maltby for mass spectrometer instrumentation advice. We thank Jan and Shokat lab members for discussion and critical reading of the manuscript. Mass spectrometry was made possible by National Institutes of Health (NIH) grants (NCRR RR015804 and NCRR RR001614). Financial support for the purchase of the Linear Trap Quadrupole (LTQ)Velos Orbitrap mass spectrometer was provided by Howard Hughes Medical Institute and an NIH grant (NCRR01614 to A.L.B.). This work was supported by the National Alliance of Schizophrenia and Depression (NARSAD) Young Investigator Award (to S.K.U.), NARSAD Distinguished Investigator Award (to Y.N.J.), Human Frontiers Science Programfellowship (to W.P.G.), NIH grants (R37NS040929 and 5R01MH084234 to Y.N.J.;RO1EB001987 to K.M.S.), and Genentech

predoctoral fellowship (to N.T.H.). K.M.S., L.Y.J., and Y.N.J. are investigators for the Howard Hughes Medical Institute.

Accepted: January 5, 2012
Published: March 21, 2012

REFERENCES

Allen, J.J., Li, M., Brinkworth, C.S., Paulson, J.L., Wang, D., Hübner, A., Chou, W.H., Davis, R.J., Burlingame, A.L., Messing, R.O., et al. (2007). A semisynthetic epitope for kinase substrates. Nat. Methods *4*, 511–516.

Bichsel, S.J., Tamaskovic, R., Stegert, M.R., and Hemmings, B.A. (2004). Mechanism of activation of NDR (nuclear Dbf2-related) protein kinase by the hMOB1 protein. J. Biol. Chem. *279*, 35228–35235.

Bishop, A.C., Ubersax, J.A., Petsch, D.T., Matheos, D.P., Gray, N.S., Blethrow, J., Shimizu, E., Tsien, J.Z., Schultz, P.G., Rose, M.D., et al. (2000). A chemical switch for inhibitor-sensitive alleles of any protein kinase. Nature *407*, 395–401.

Blethrow, J.D., Glavy, J.S., Morgan, D.O., and Shokat, K.M. (2008). Covalent capture of kinase-specific phosphopeptides reveals Cdk1-cyclin B substrates. Proc. Natl. Acad. Sci. USA *105*, 1442–1447.

Brondyk, W.H., McKiernan, C.J., Fortner, K.A., Stabila, P., Holz, R.W., and Macara, I.G. (1995). Interaction cloning of Rabin3, a novel protein that associates with the Ras-like GTPase Rab3A. Mol. Cell. Biol. *15*, 1137–1143.

Brown, T.C., Correia, S.S., Petrok, C.N., and Esteban, J.A. (2007). Functional compartmentalization of endosomal trafficking for the synaptic delivery of AMPA receptors during long-term potentiation. J. Neurosci. *27*, 13311–13315.

Cong, J., Geng, W., He, B., Liu, J., Charlton, J., and Adler, P.N. (2001). The furry gene of Drosophila is important for maintaining the integrity of cellular extensions during morphogenesis. Development *128*, 2793–2802.

Conner, S.D., and Schmid, S.L. (2002). Identification of an adaptor-associated kinase, AAK1, as a regulator of clathrin-mediated endocytosis. J. Cell Biol. *156*, 921–929.

Conner, S.D., and Schmid, S.L. (2003). Differential requirements for AP-2 in clathrin-mediated endocytosis. J. Cell Biol. *162*, 773–779.

Cornils, H., Stegert, M.R., Hergovich, A., Hynx, D., Schmitz, D., Dirnhofer, S., and Hemmings, B.A. (2010). Ablation of the kinase NDR1 predisposes mice to the development of T cell lymphoma. Sci. Signal. *3*, ra47.

Cornils, H., Kohler, R.S., Hergovich, A., and Hemmings, B.A. (2011). Human NDR kinases control G(1)/S cell cycle transition by directly regulating p21 stability. Mol. Cell. Biol. *31*, 1382–1395.

De Matteis, M.A., Di Campli, A., and Godi, A. (2005). The role of the phosphoinositides at the Golgi complex. Biochim. Biophys. Acta *1744*, 396–405.

Devroe, E., Erdjument-Bromage, H., Tempst, P., and Silver, P.A. (2004). Human Mob proteins regulate the NDR1 and NDR2 serine-threonine kinases. J. Biol. Chem. *279*, 24444–24451.

Emoto, K., He, Y., Ye, B., Grueber, W.B., Adler, P.N., Jan, L.Y., and Jan, Y.N. (2004). Control of dendritic branching and tiling by the Tricornered-kinase/Furry signaling pathway in Drosophila sensory neurons. Cell *119*, 245–256.

Emoto, K., Parrish, J.Z., Jan, L.Y., and Jan, Y.N. (2006). The tumour suppressor Hippo acts with the NDR kinases in dendritic tiling and maintenance. Nature *443*, 210–213.

Fiala, J.C., Feinberg, M., Popov, V., and Harris, K.M. (1998). Synaptogenesis via dendritic filopodia in developing hippocampal area CA1. J. Neurosci. *18*, 8900–8911.

Gallegos, M.E., and Bargmann, C.I. (2004). Mechanosensory neurite termination and tiling depend on SAX-2 and the SAX-1 kinase. Neuron *44*, 239–249.

Geng, W., He, B., Wang, M., and Adler, P.N. (2000). The tricornered gene, which is required for the integrity of epidermal cell extensions, encodes the Drosophila nuclear DBF2-related kinase. Genetics *156*, 1817–1828.

Gerges, N.Z., Backos, D.S., and Esteban, J.A. (2004). Local control of AMPA receptor trafficking at the postsynaptic terminal by a small GTPase of the Rab family. J. Biol. Chem. *279*, 43870–43878.

Gupta-Rossi, N., Ortica, S., Meas-Yedid, V., Heuss, S., Moretti, J., Olivo-Marin, J.C., and Israël, A. (2011). The adaptor-associated kinase 1, AAK1, is a positive regulator of the Notch pathway. J. Biol. Chem. *286*, 18720–18730.

Han, C., Wang, D., Soba, P., Zhu, S., Lin, X., Jan, L.Y., and Jan, Y.N. (2012). Integrins regulate repulsion-mediated dendritic patterning of drosophila sensory neurons by restricting dendrites in a 2D space. Neuron *73*, 64–78.

Harris, K.M. (1999). Structure, development, and plasticity of dendritic spines. Curr. Opin. Neurobiol. *9*, 343–348.

Hattula, K., Furuhjelm, J., Arffman, A., and Peränen, J. (2002). A Rab8-specific GDP/GTP exchange factor is involved in actin remodeling and polarized membrane transport. Mol. Biol. Cell *13*, 3268–3280.

Henderson, D.M., and Conner, S.D. (2007). A novel AAK1 splice variant functions at multiple steps of the endocytic pathway. Mol. Biol. Cell *18*, 2698–2706.

Hergovich, A., Stegert, M.R., Schmitz, D., and Hemmings, B.A. (2006). NDR kinases regulate essential cell processes from yeast to humans. Nat. Rev. Mol. Cell Biol. *7*, 253–264.

Hertz, N.T., Wang, B.T., Allen, J.J., Zhang, C., Dar, A.C., Burlingame, A.L., and Shokat, K.M. (2010). Chemical genetic approach for kinase-substrate mapping by covalent capture of thiophosphopeptides and analysis by mass spectrometry. Curr Protoc Chem Biol. *V2*, 15–36.

Horgan, C.P., and McCaffrey, M.W. (2009). The dynamic Rab11-FIPs. Biochem. Soc. Trans. *37*, 1032–1036.

Horton, A.C., Rácz, B., Monson, E.E., Lin, A.L., Weinberg, R.J., and Ehlers, M.D. (2005). Polarized secretory trafficking directs cargo for asymmetric dendrite growth and morphogenesis. Neuron *48*, 757–771.

Jan, Y.N., and Jan, L.Y. (2010). Branching out: mechanisms of dendritic arborization. Nat. Rev. Neurosci. *11*, 316–328.

Jansen, J.M., Wanless, A.G., Seidel, C.W., and Weiss, E.L. (2009). Cbk1 regulation of the RNA-binding protein Ssd1 integrates cell fate with translational control. Curr. Biol. *19*, 2114–2120.

Koike-Kumagai, M., Yasunaga, K., Morikawa, R., Kanamori, T., and Emoto, K. (2009). The target of rapamycin complex 2 controls dendritic tiling of Drosophila sensory neurons through the Tricornered kinase signalling pathway. EMBO J. *28*, 3879–3892.

Konur, S., and Yuste, R. (2004). Developmental regulation of spine and filopodial motility in primary visual cortex: reduced effects of activity and sensory deprivation. J. Neurobiol. *59*, 236–246.

Kuai, L., Ong, S.E., Madison, J.M., Wang, X., Duvall, J.R., Lewis, T.A., Luce, C.J., Conner, S.D., Pearlman, D.A., Wood, J.L., et al. (2011). AAK1 identified as an inhibitor of neuregulin-1/ErbB4-dependent neurotrophic factor signaling using integrative chemical genomics and proteomics. Chem. Biol. *18*, 891–906.

Kuo, C.T., Zhu, S., Younger, S., Jan, L.Y., and Jan, Y.N. (2006). Identification of E2/E3 ubiquitinating enzymes and caspase activity regulating Drosophila sensory neuron dendrite pruning. Neuron *51*, 283–290.

Kurischko, C., Kuravi, V.K., Wannissorn, N., Nazarov, P.A., Husain, M., Zhang, C., Shokat, K.M., McCaffery, J.M., and Luca, F.C. (2008). The yeast LATS/Ndr kinase Cbk1 regulates growth via Golgi-dependent glycosylation and secretion. Mol. Biol. Cell *19*, 5559–5578.

Li, Z., Jo, J., Jia, J.M., Lo, S.C., Whitcomb, D.J., Jiao, S., Cho, K., and Sheng, M. (2010). Caspase-3 activation via mitochondria is required for long-term depression and AMPA receptor internalization. Cell *141*, 859–871.

MacVicar, B.A., and Thompson, R.J. (2010). Non-junction functions of pannexin-1 channels. Trends Neurosci. *33*, 93–102.

Matsuzaki, M., Ellis-Davies, G.C., Nemoto, T., Miyashita, Y., Iino, M., and Kasai, H. (2001). Dendritic spine geometry is critical for AMPA receptor expression in hippocampal CA1 pyramidal neurons. Nat. Neurosci. *4*, 1086–1092.

Mazanka, E., Alexander, J., Yeh, B.J., Charoenpong, P., Lowery, D.M., Yaffe, M., and Weiss, E.L. (2008). The NDR/LATS family kinase Cbk1 directly controls transcriptional asymmetry. PLoS Biol. *6*, e203.

Millward, T.A., Hess, D., and Hemmings, B.A. (1999). Ndr protein kinase is regulated by phosphorylation on two conserved sequence motifs. J. Biol. Chem. *274*, 33847–33850.

Nelson, B., Kurischko, C., Horecka, J., Mody, M., Nair, P., Pratt, L., Zougman, A., McBroom, L.D., Hughes, T.R., Boone, C., and Luca, F.C. (2003). RAM: a conserved signaling network that regulates Ace2p transcriptional activity and polarized morphogenesis. Mol. Biol. Cell *14*, 3782–3803.

Nimchinsky, E.A., Sabatini, B.L., and Svoboda, K. (2002). Structure and function of dendritic spines. Annu. Rev. Physiol. *64*, 313–353.

Penzes, P., Cahill, M.E., Jones, K.A., VanLeeuwen, J.E., and Woolfrey, K.M. (2011). Dendritic spine pathology in neuropsychiatric disorders. Nat. Neurosci. *14*, 285–293.

Ramocki, M.B., and Zoghbi, H.Y. (2008). Failure of neuronal homeostasis results in common neuropsychiatric phenotypes. Nature *455*, 912–918.

Robinson, M.S. (2004). Adaptable adaptors for coated vesicles. Trends Cell Biol. *14*, 167–174.

Sekiya-Kawasaki, M., Groen, A.C., Cope, M.J., Kaksonen, M., Watson, H.A., Zhang, C., Shokat, K.M., Wendland, B., McDonald, K.L., McCaffery, J.M., and Drubin, D.G. (2003). Dynamic phosphoregulation of the cortical actin cytoskeleton and endocytic machinery revealed by real-time chemical genetic analysis. J. Cell Biol. *162*, 765–772.

Shah, K., Liu, Y., Deirmengian, C., and Shokat, K.M. (1997). Engineering unnatural nucleotide specificity for Rous sarcoma virus tyrosine kinase to uniquely label its direct substrates. Proc. Natl. Acad. Sci. USA *94*, 3565–3570.

Stegert, M.R., Tamaskovic, R., Bichsel, S.J., Hergovich, A., and Hemmings, B.A. (2004). Regulation of NDR2 protein kinase by multi-site phosphorylation and the S100B calcium-binding protein. J. Biol. Chem. *279*, 23806–23812.

Stegert, M.R., Hergovich, A., Tamaskovic, R., Bichsel, S.J., and Hemmings, B.A. (2005). Regulation of NDR protein kinase by hydrophobic motif phosphorylation mediated by the mammalian Ste20-like kinase MST3. Mol. Cell. Biol. *25*, 11019–11029.

Stenmark, H. (2009). Rab GTPases as coordinators of vesicle traffic. Nat. Rev. Mol. Cell Biol. *10*, 513–525.

Stork, O., Zhdanov, A., Kudersky, A., Yoshikawa, T., Obata, K., and Pape, H.C. (2004). Neuronal functions of the novel serine/threonine kinase Ndr2. J. Biol. Chem. *279*, 45773–45781.

Toshima, J., Toshima, J.Y., Martin, A.C., and Drubin, D.G. (2005). Phosphoregulation of Arp2/3-dependent actin assembly during receptor-mediated endocytosis. Nat. Cell Biol. *7*, 246–254.

Vichalkovski, A., Gresko, E., Cornils, H., Hergovich, A., Schmitz, D., and Hemmings, B.A. (2008). NDR kinase is activated by RASSF1A/MST1 in response to Fas receptor stimulation and promotes apoptosis. Curr. Biol. *18*, 1889–1895.

Wang, Z., Edwards, J.G., Riley, N., Provance, D.W., Jr., Karcher, R., Li, X.D., Davison, I.G., Ikebe, M., Mercer, J.A., Kauer, J.A., and Ehlers, M.D. (2008). Myosin Vb mobilizes recycling endosomes and AMPA receptors for postsynaptic plasticity. Cell *135*, 535–548.

Williams, D.W., Kondo, S., Krzyzanowska, A., Hiromi, Y., and Truman, J.W. (2006). Local caspase activity directs engulfment of dendrites during pruning. Nat. Neurosci. *9*, 1234–1236.

Yang, W.K., Peng, Y.H., Li, H., Lin, H.C., Lin, Y.C., Lai, T.T., Suo, H., Wang, C.H., Lin, W.H., Ou, C.Y., et al. (2011). Nak regulates localization of clathrin sites in higher-order dendrites to promote local dendrite growth. Neuron *72*, 285–299.

Ye, B., Zhang, Y., Song, W., Younger, S.H., Jan, L.Y., and Jan, Y.N. (2007). Growing dendrites and axons differ in their reliance on the secretory pathway. Cell *130*, 717–729.

Yuste, R., and Bonhoeffer, T. (2004). Genesis of dendritic spines: insights from ultrastructural and imaging studies. Nat. Rev. Neurosci. *5*, 24–34.

Zhang, C., Kenski, D.M., Paulson, J.L., Bonshtien, A., Sessa, G., Cross, J.V., Templeton, D.J., and Shokat, K.M. (2005). A second-site suppressor strategy for chemical genetic analysis of diverse protein kinases. Nat. Methods *2*, 435–441.